JOURNAL OF MATERIALS SCIENCE 24 (1989) 2065–2070

The microstructure and mechanical properties of unidirectionally solidified Al–Si alloys

F. YILMAZ
Department of Metallurgy, Engineering Faculty of Sakarya, I.T.U., Sakarya, Turkey
R. ELLIOTT
Department of Metallurgy and Materials Science, University of Manchester, England

Hypereutectic Al–Si alloys with minor additions of Sr were directionally solidified with a temperature gradient of 125° C cm^{-1} in the liquid. Silicon in the range 14–17 wt%, Sr in the range 0.0–0.5 wt% and specimen traction velocities between 1 and 1500 μm sec^{-1} were used. The relationship between hardness and traction velocity and spacing in eutectic silicon morphologies is defined and shown to be of the same form as that for yield stress. The possibility of using hardness measurements to indicate mechanical properties is discussed. The complex regular silicon structure makes a significant contribution to the hardness of hypereutectic alloys. This makes the relationship between hardness and traction velocity more complex adding difficulties to the use of hardness to measure mechanical properties.

1. Introduction

Considerable effort has been directed in recent years to the development and characterization of *in situ* composites. Several studies have related structure and mechanical properties in directionally solidified Al–12.6 wt% Si alloys and analysed their mechanical properties in terms of composite behaviour [1–4]. For example, Justi and Bragg [1, 2] have demonstrated a Hall–Petch type of behaviour described by

$$\sigma_{YS} = \sigma_0 + K_1\lambda^{-0.5} \quad (1)$$

and as for eutectics,

$$\lambda^2 v = K_2 \quad (2)$$

$$\sigma_{YS} = \sigma_0 + K_3 v^{+0.25} \quad (3)$$

where σ_{YS} is yield stress, σ_0 is yield stress for matrix, λ is interphase spacing, v is growth velocity and K_1, K_2 and K_3 are constants. This relationship was observed for growth velocities (v) less than about 5 μm sec^{-1} when the silicon phase of the eutectic forms branched rods or the angular silicon structure (Fig. 1a). The silicon phase grows as flakes at higher growth velocities and a small but constant increase in strength was observed with increasing growth velocity. This study demonstrated that hardness measurements can be used as a reliable indicator of mechanical properties. Hardness measurements showed the same dependence on growth velocity as yield stress. A ratio of 0.13 was suggested for converting hardness into yield stress (kg mm^{-2}) and a ratio of 0.3 for conversion into ultimate tensile strength. The shaded points in Fig. 2 show the variation of hardness with growth velocity reported by Justi and Bragg. Recently Telli and Kisakurek [4] have presented measurements for the flake eutectic. Their hardness and tensile measurements show the same variation with growth velocity. However, Fig. 2 shows that their hardness measurements do not obey Equation 3. Their spacing measurements do not follow Equation 2 but, as shown in Fig. 5, Equation 1 is obeyed and is suggested as the basis for mechanical property assessment from spacing measurements.

We have recently completed a comprehensive study of the various silicon growth modes that occur during directional solidification covering a wide range of growth velocities, silicon and Sr concentrations [5, 6]. We have made hardness measurements on transverse sections of a selection of these specimens in order to resolve some of the discrepancies in the previous measurements. The previous measurements of Justi and Bragg [1, 2] are confirmed and extended to define the relationship between hardness, growth velocity and silicon particle spacing for different silicon growth modes to ascertain whether there is a basis for using hardness measurements to indicate mechanical properties.

2. Experimental procedure

Some 100 specimens covering the composition range 14–17 wt % Si were prepared using metals of 99.999% purity. Weighed amounts of aluminium and silicon were melted under argon and after melt homogenization were sucked into alumina tubes 30 cm long and 6 mm o.d. The melt remaining was quenched and used for silicon analysis. Sr in the form of an Al–1.2 wt % Sr master alloy was added to selected alloys in small concentrations up to 0.05 wt %. These alloys were prepared in the same way and the quenched melt was analysed for silicon and Sr. All alloys were remelted in a vertical Bridgeman directional solidification apparatus and after allowing time for melt stabilization were solidified by withdrawing the specimen into a water cooled, water reservoir at a constant traction

0022–2461/89 $03.00 + .12

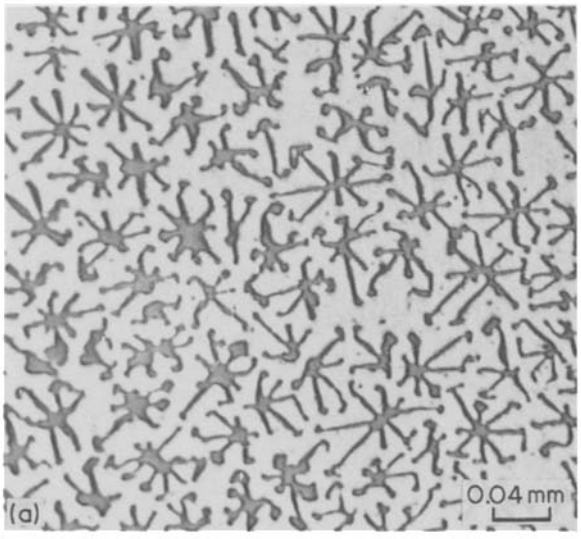

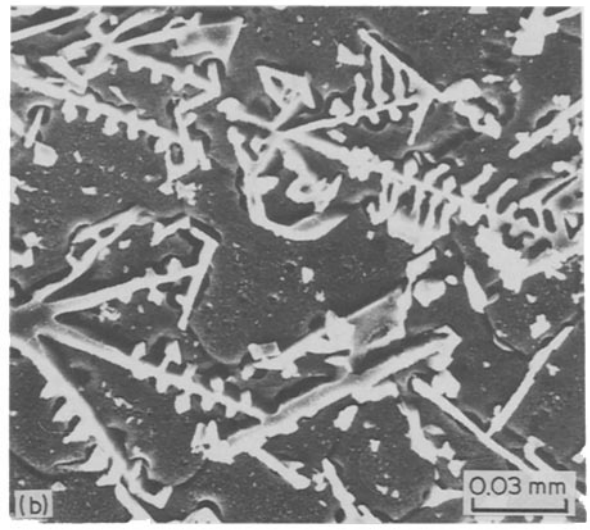

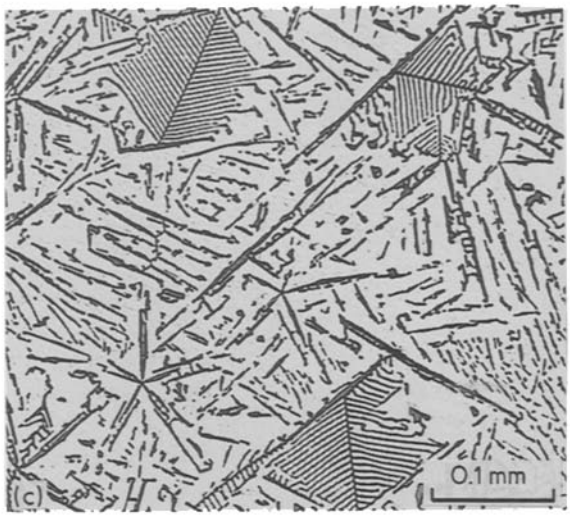

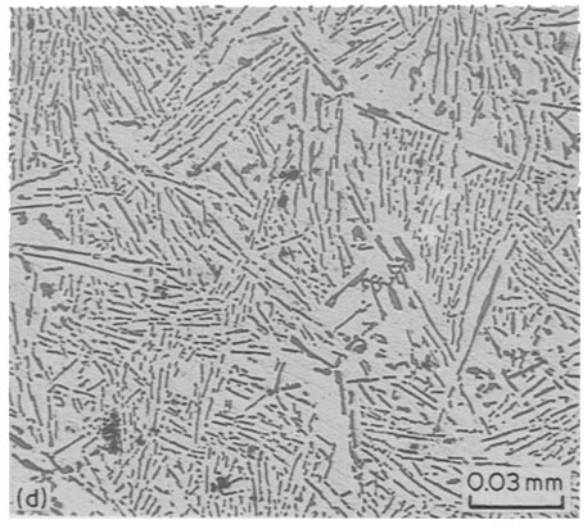

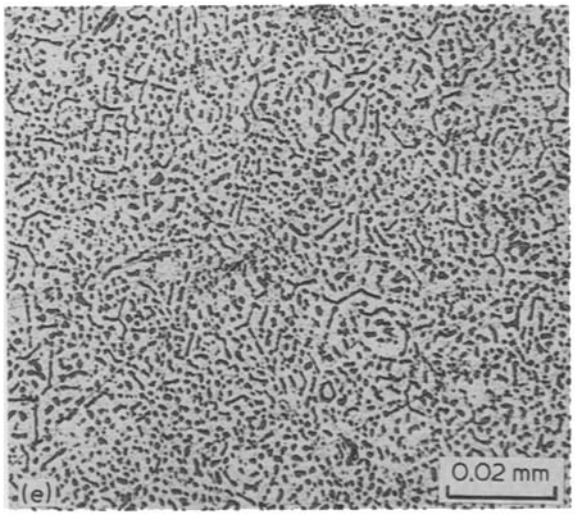

Figure 1 (a) Angular silicon crystals developed from silicon rods. Transverse section of an Al–15 wt % Si alloy, growth velocity 1.5 μm sec^{-1}. (b) The formation of complex regular lamellae on angular silicon side plates in an Al–15 wt % Si alloy, growth velocity 1.8 μm sec^{-1}. (c) Flake eutectic, complex regular and star-like silicon in a transverse section of an Al–15.75 wt % Si alloy, growth velocity 10 μm sec^{-1}. (d) Flake eutectic in a transverse section of an Al–15 wt % Si alloy, growth velocity 103 μm sec^{-1}. (e) Angular silicon and fibrous eutectic in a transverse section of an Al–17 wt % Si–0.048 wt % Sr alloy, growth velocity 100 μm sec^{-1}.

rate in the range 1–1500 μm sec^{-1}. Fine thermocouples embedded in the specimen measured a temperature gradient of 125 $\pm$ 5° C cm^{-1} for the furnace temperature used. Analysis of direct cooling curves [7] shows that the traction velocity and interface velocity are equal for traction velocities up to 100 μm sec^{-1} but the growth velocity falls behind the traction velocity at higher velocities. Longitudinal and transverse sections were polished for optical microscopy and deeply etched in HCl for scanning electron microscopy. The volume fraction of complex regular silicon phase was measured from these sections. A linear intercept method was used to measure average eutectic flake spacing and the lamellar spacing in the complex regular structure from transverse sections. Interfibre spacing was measured from a photograph of a transverse section of magnification, M, by counting the number of fibres, N, within a known area, A. The average interfibre spacing was calculated from

$$\lambda = \frac{1}{M}\left(\frac{A}{N}\right)^{1/2} \quad (4)$$

Finally, micro- and macro-hardness measurements were made on selected areas of transverse sections using a Leitz and Karl Frank GMCH hardness tester, respectively.

3. Experimental results and discussion

Figure 3 shows the different silicon phase morphologies

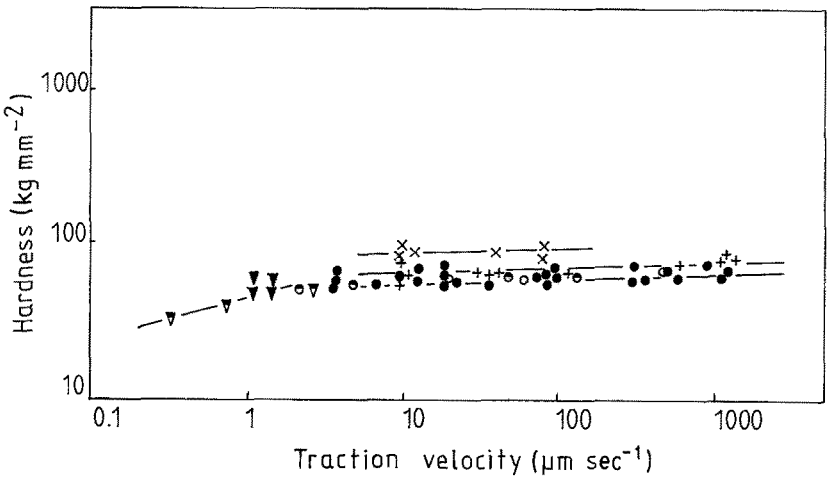

Figure 2 The variation of microhardness with traction velocity: (▼) angular Si (Justi and Bragg [1, 2]); (▽) angular Si (present study); (◓) flake Si (Justi and Bragg [1, 2]); (○) flake Si (Telli and Kisakurek [4]); (●) flake Si (present study); (+) fibrous Si (present study); (×) complex regular (present study).

observed in directionally solidified hypereutectic Al–Si alloys. Alloys containing between 14 and 17 wt % Si were used in order to produce eutectic structures without aluminium primary phase formation over a wide range of growth velocities, and to extend the measurements to hypereutectic Al–Si alloys. The most commonly occurring morphology is the interconnected eutectic flake silicon structure. Quench modified fibrous eutectic silicon occurs increasingly as the growth velocity exceeds 500 μm sec^{-1} and impurity modified fibrous eutectic silicon in the presence of Sr. The complex regular morphology occupies up to 30% by volume depending on the silicon concentration and solidification conditions. The different silicon morphologies are shown in Fig. 1.

Interparticle spacing measurements for the coupled growth modes, flake, fibrous and complex regular are given in Table I and plotted against traction velocity in Fig. 4. Spacing values for the angular silicon structure computed for temperature gradients of 80 and 125° C cm^{-1} from previous measurements are shown in Fig. 4. There is scatter in the flake spacings because of the nature of this growth form, and in the fibrous structure because of its sensitivity to Sr content. There is considerably less scatter in the complex regular structure because of the regularity of this structure.

Each of these relationships can be described by an equation of the form

$$\lambda = K_4 v^{-n} \quad (5)$$

where n varies between 0.39 and 0.45. Bearing in mind that the traction velocity exceeds the growth velocity for traction velocities in excess of 100 μm sec^{-1}, it is considered that the spacing measurements for each silicon morphology can be described by an equation of the form

$$\lambda = K_5 v^{-0.5} \quad (6)$$

The corrected velocities are shown by the filled circles for the complex regular structure in Fig. 4. The value of n measured by Telli and Kisakurek [4] was 0.11. This is considerably smaller than the value recorded in all other studies.

Microhardness measurements made on flake, fibrous and complex regular areas of transverse sections are recorded in Table II. They are shown as a function of traction velocity in Fig. 2. The present measurements confirm that the behaviour of specimens with the angular silicon structure can be described by Equation 3. They confirm the limited number of measurements made by Justi and Bragg for the flake structure and show that hardness and traction velocity are related

TABLE I Mean interparticle spacing measurements for different eutectic morphologies

Traction velocity (μm sec^{-1})	Flake spacing (μm) 0.00% Sr–16.97% Si	Fibre spacing (μm) 0.025% Sr–17.10% Si	Fibre spacing (μm) 0.048% Sr–17.10% Si	Complex regular spacing (μm) 0.00% Sr–15.75% Si
10.0				3.91
15.8		4.84	4.25	
24.3	5.53			2.68
27.3			3.01	
40.0				2.27
51.8		3.43	2.39	
100.0		2.43	2.13	
103.0	3.16			1.34
193.0		2.09		
259.0				1.00
349.0	1.58			0.79
517.0				0.67
553.0		1.21		
794.0				0.59
951.0	1.23			
1218.0	1.02*			

*Semi-fibrous.

TABLE II Hardness as a function of traction velocity for different silicon morphologies

Traction velocity ($\mu m\,sec^{-1}$)	Complex regular hardness ($kg\,mm^{-2}$)	Fibrous hardness ($kg\,mm^{-2}$)	Flake hardness ($kg\,mm^{-2}$)
1.09		50 63*	
1.44		50*	
1.51		60*	
3.80			53 60 69
9.10		55	65
9.50		76	
10.00	87 95		
11.00		60	
12.60	87		58 66
18.20			55 63 73
22.90			58
30.20		68	
36.30		60	55
38.00	93		
45.90		56	
47.80		63	
72.40			60
83.00			65
87.00			58
99.00			63 71
120.00		60	
288.00			58 73
363.00			58
524.00			73
575.00			62
645.00		73	
912.00			72
1096.00		74	
1174.00		85	62†
1318.00		79	

*Angular silicon.
†Fibrous.

by an equation of the form

$$H = H_0 + K_6 v^n \quad (7)$$

where n is 0.04. Telli and Kisakurek's results show a similar behaviour. The deviation from Equation 3 is not surprising in view of the considerable branching and misalignment of the flake silicon compared to the silicon rods in the angular silicon structure. Although there is scatter in the hardness measurements for the flake and fibrous silicon structures separate relationships of a similar form can be used to describe the measurements in Fig. 2 in keeping with the higher tensile strength displayed by the fibrous eutectic. The complex regular structure can be represented by a similar relationship as shown in Fig. 2. The results in Tables I and II can be combined to give the hardness–interparticle spacing relationships shown in Fig. 5. The present measurements can be represented by an equation of the form

$$H = H_0 + K_7 \lambda^{-n} \quad (8)$$

where $n = 0.5$ for the angular silicon structure and 0.08 for the flake, fibrous and complex regular silicon structures. The yield stress measurements due to Justi and Bragg [1, 2] for flake eutectic silica are shown in Fig. 5. They exhibit a similar dependence on spacing to that found for hardness in the present study. The hardness and yield stress measurements made by Telli and Kisakurek [4] and found to obey Equation 1 are shown in the same figure. Thus the present results show that hardness exhibits a well defined relationship to spacing similar to that observed for yield stress and this relationship can form the basis for a method of indicating mechanical properties. In agreement with the findings of Justi and Bragg, and contrary to those of Telli and Kisakurek, a Hall–Petch type of relationship was found only for the angular silicon structure.

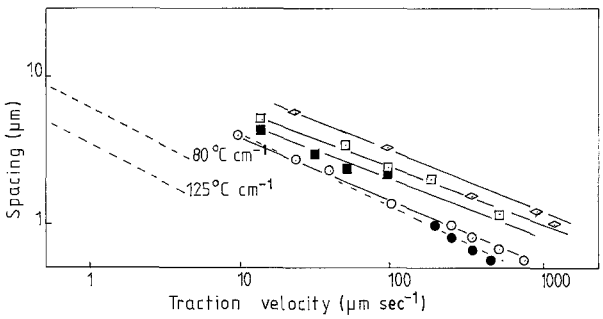

Figure 4 The variation of mean interparticle spacing with traction velocity measured on transverse sections. (◇) 16.97 wt % Si, 0.00 wt % Sr, flake Si; (□) 17.10 wt % Si, 0.025 wt % Sr, fibrous Si; (■) 17.10 wt % Si, 0.048 wt % Sr, fibrous Si; (○) 15.75 wt % Si, 0.00 wt % Sr, complex regular Si; (– – –) computed for angular Si structure.

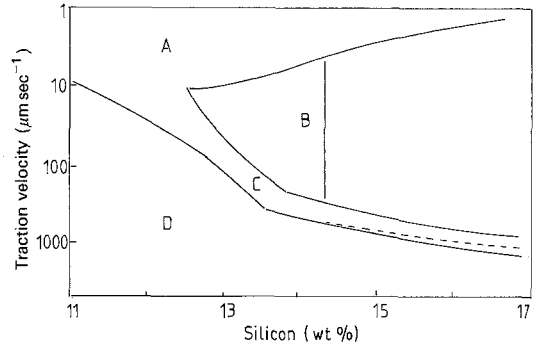

Figure 3 The relationship between structure, silicon composition and traction velocity: Region A – angular, rod and flake eutectic silicon; region B – eutectic, complex regular, star-like and octahedral primary Si [Si > 14.5%]; region C – eutectic Si, primary Si [Si > 14.5%]; region D – α-Al dendrites, eutectic Si and primary phase [Si > 14.5%]. The dotted line in region C shows the flake–fibre transition.

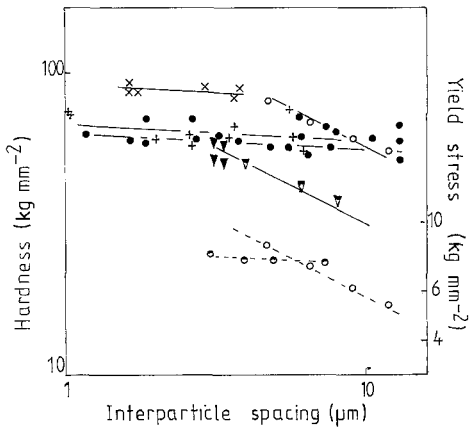

Figure 5 Hardness (——) and yield stress (– – –) measurements as a function of interparticle spacing for different silicon structures. Symbols are the same as in Fig. 2.

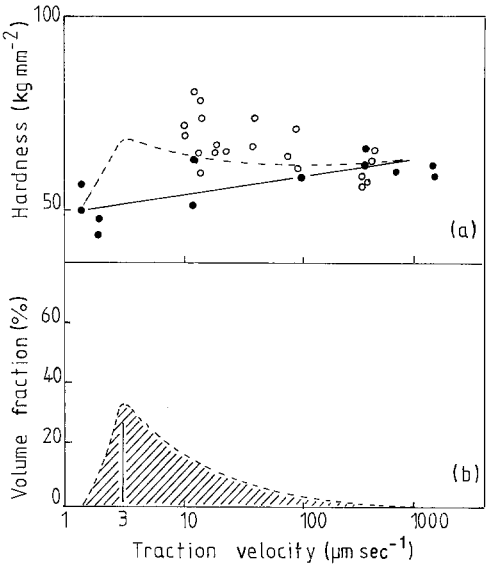

Figure 6 (a) The variation of macrohardness with traction velocity: (●) angular Si and fibrous Si (Al–Si–Sr alloys); (○) complex regular and flake Si (Al–Si alloys); (– – –) calculated using the rule of mixtures. (b) The variation of complex regular silicon volume fraction with traction velocity in an Al–17 wt % Si alloy.

Many Al–Si casting alloys are of hypereutectic composition. In order to assess the possibility of using hardness measurements in such alloys macrohardness measurements were made on alloys containing 15–17 wt % Si with and without Sr. The measurements are recorded in Table III and plotted in Fig. 6. Two relationships are evident. Alloys containing Sr show a linear dependence of hardness on traction velocity. This dependence is the same as that recorded by microhardness measurements shown in Fig. 2 for the fibrous eutectic structure. The addition of Sr to the hypereutectic alloys promotes the fibrous eutectic morphology. Alloys without Sr show a mixed structure of eutectic silicon, complex regular silicon, star-like silicon and polyhedral primary silicon as shown in Fig. 1c. The last two morphologies occupy a very small volume fraction of the structure in the pure alloys used in the present study. Only eutectic flake and complex regular silicon structures are considered

TABLE III Macrohardness measurements on 15–17 wt % Si alloys with and without Sr

Traction velocity (μm sec^{-1})	Macrohardness (kg mm^{-2})	
	Complex regular + flake eutectic (15–17% Si)	Fibrous eutectic + angular silicon 15–17% Si–0.02–0.05% Sr
1.50		50 54
1.90		44 47
10.00	65 65	
11.80		49 59
13.10	73 76	
13.20	54 59 70	
19.70	61 63	
23.70	61 61	
39.50	61 70	
79.00	61 70	
95.00	56	
98.90		55 55
317.00	52 54 55	59 63
380.00	59 61	
1267.00		55 57

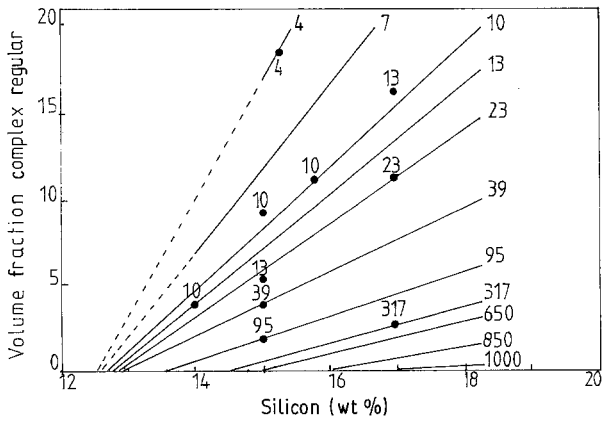

Figure 7 The variation of complex regular silicon volume fraction with silicon composition. The numbers indicate growth velocity (μm sec^{-1}). The circles are experimental measurements.

in analysing the non linear relationship in Fig. 6. This relationship may be predicted using a rule of mixtures of the form alloy hardness = eutectic hardness × V_F + complex regular hardness × (1 − V_F) where V_F is the volume fraction of eutectic and the hardness of the eutectic and complex regular silicon is defined in Fig. 2. The complex regular silicon phase is present in region B in Fig. 3 in amounts that depend on the silicon concentration and growth velocity for a constant temperature gradient in the liquid. The upper and lower boundaries in region B in Fig. 3 define the conditions under which complex regular silicon phase forms in unmodified alloys. These boundaries are evident in Fig. 7 which shows measured volume fractions of complex regular silicon phase in directionally solidified alloys. The hardness curve calculated on the basis of the rule of mixtures is shown by the dashed curve in Fig. 6 and is of a similar form to that measured. Fig. 6b shows the change in complex regular volume fraction with traction velocity in a 17 wt % Si alloy. The critical growth velocity of $\sim 3\,\mu$m sec^{-1} is recognized as the velocity above which twinning occurs in silicon. The eutectic silicon phase forms as branched rods or angular silicon by a dislocation growth mechanism at velocities below this value. The TPRE (twin plane re-entrant edge) mechanism of growth operates above this velocity and the eutectic phase is either flake or fibres. At velocities close to the critical value neither mechanism is fully operative and complex regular silicon growth occurs connecting {1 0 0} angular silicon plates and {1 1 1} flakes as shown in Fig. 1b. The conditions used in the present study are simple, in that, the high temperature gradient suppresses complex regular silicon formation and silicon nucleation. However, the relationship between hardness and growth velocity is no longer linear. The solidification of castings usually occurs under lower temperature gradients and with inoculants added to promote silicon nucleation. It can be anticipated that several silicon morphologies are likely to be formed and the relationship between hardness and velocity is likely to be more complex.

4. Conclusions

The present results show that the hardness of eutectic silicon morphologies exhibit well defined relationships

with silicon particle spacing that is of a similar form to that between yield stress and spacing suggesting that hardness may be used to indicate mechanical strength. A more complex relationship that is sensitive to solidification conditions was found in hypereutectic alloys suggesting that the use of hardness to indicate mechanical properties is more complicated. Whether a single hardness–spacing relationship can be used to describe flake structures for all solidification conditions (different temperature gradients and in the presence of solutes like Sb that refine the flake structure) as suggested by Telli and Kisakurek [4] or indeed, whether a single relationship may be used to describe flake and fibrous (Sr modified) eutectic structures will be considered further when structural and mechanical property measurements on a range of alloys have been completed.

References

1. S. JUSTI and R. H. BRAGG, *Met. Trans. AIME* **7A** (1975) 1954.
2. *Idem, ibid.* **9A** (1978) 515.
3. M. SAHOO and R. W. SMITH, *Metal. Sci. J.* **9** (1975) 217.
4. A. I. TELLI and S. E. KISAKUREK, *Mat. Sci. Techn.* **4** (1988) 153.
5. O. A. ATASOY, F. YILMAZ and R. ELLIOTT, *J. Cryst. Growth* **66** (1984) 137.
6. F. YILMAZ, O. A. ATASOY and R. ELLIOTT, *J. Cryst. Growth*, to be published.
7. R. ELLIOTT, *Met. Trans.*, to be published.

Received 24 March
and accepted 29 July 1988